Development of a Novel Markov Chain Model for the Prediction of Head and Neck Squamous Cell Carcinoma Dissemination

Hyunggu Jung, MS, MMath[1], Anthony Law, MD, PhD[2], Eli Grunblatt[3], Lucy L. Wang, MS[1], Aaron Kusano, MD, MS[4], Jose L. V. Mejino Jr., MD[5], Mark E. Whipple, MD, MS[1,2]

[1]Department of Biomedical Informatics and Medical Education
[2]Department of Otolaryngology-Head and Neck Surgery
[3]Medical Scientist Training Program
[4]Department of Radiation Oncology
[5]Department of Biological Structure
University of Washington, Seattle, WA

Abstract

Prediction of microscopic tumor spread to regional lymph nodes can assist in radiation planning for cancer treatment. However, it is still challenging to predict tumor spread. In this paper, we present a unique approach to modeling how tumor cells disseminate to form regional metastases. This involves leveraging well established knowledge resources and commonly held notions of how cancer spreads. Using patient data, we utilized our approach to create a model of metastasis for the subset of head and neck squamous cell carcinoma that arises in the mucosa of the lateral tongue. The model was created using a training set extracted from the clinical records of 50 patients with tumors of this type who presented to the University of Washington head and tumor board over a three and half year period. The test sets consist of four case series drawn from the literature.

Introduction

Head and neck squamous cell carcinoma (HNSCC) is the most common form of cancer of the upper aerodigestive tract. The mainstays of treatment consist of surgery and/or radiation therapty. Radiation therapy involves identifying the target region in the patient (the neoplastic area requiring treatment) and then customizing a treatment plan that achieves a therapeutic dose of radiation to this zone while minimizing the dose to the surrounding area. Reports from the International Commission on Radiation Units and Measurements (ICRU)[1, 2] define several kinds of volumes to guide radiotherapy planning. The Gross Tumor Volume (GTV) is defined as "the gross palpable or visible/demonstrable extent and location of malignant growth." The GTV is typically defined using computer drawing tools on computed tomography (CT) or other imaging modalities by an attending physician. Even with the best imaging technique, the boundaries of such a volume may be very uncertain, and much clinical judgement is involved. The Clinical Target Volume (CTV) is defined as the volume that includes the GTV and/or microscopic malignant disease. At present, the radiation oncologist uses his/her knowledge of the pathology literature, clinical experience and knowledge of anatomy to draw the CTV. This leaves much room for improvement, in particular in the ability to predict the extent of subclinical microscopic disease.

Prediction of microscopic spread of tumor cells is becoming critically important in the decision making process of planning radiation therapy for cancer. Until relatively recently, standard radiation treatment of HNSCC incorporated relatively large treatment areas. With the onset of Intensity Modulated Radiation Therapy (IMRT), treatment can be more precisely applied, such that if it is known that regional spread is confined to a specific set of lymph nodes, a more focused treatment can be considered. The resultant payoff is reducing or eliminating the collateral damage due to over-irradiation of surrounding tissue. Imaging methods such as CT or magnetic resonance imaging (MRI) can only show evidence of gross disease that has caused enlargement of the lymph nodes. Functional scans, such as positron emission tomography (PET), can demonstrate smaller metastases, but even with PET imaging it is not possible to determine with certainty whether nodes are involved and should be treated.[7] None of these imaging modalities can detect micro-metastases, which can currently only be confirmed post-surgery by pathologic evaluations of surgical specimens.

The initial work on this project[8, 9] showed that a model of tumor dissemination based on an anatomy ontology and some simple assumptions can produce predictions that have a fair agreement with published surgical data. The modeling strategy uses the idea of a Markov chain. Each lymphatic chain[1] can be described in terms of the probability

[1]We are using the term "chain" in two ways here. A lymphatic chain is so called because it typically consists of a series of vessels connecting several lymph nodes in a linear string. That unit as a whole is modeled as a Markov chain, meaning its state is represented as a stochastic process, or sequence over time.

for it to be in any of five possible states, numbered 0 through 4. State 0 means no tumors present. State 1 means a little tumor, state 2 somewhat more, and so on, to state 4 which is a big palpable node. The only way a lymphatic chain can go from state 0 to state 1 is by some tumor cells migrating downstream from the upstream chain, but once some tumor cells are there, they can transition to the states of larger growth on their own. The simplest way to think about the spread of tumor cells is to imagine that the process happens in discrete time steps. The tumor is in some initial state, and each lymphatic chain is as well. The states change with each time step.

The idea of a Markov chain is that a system can undergo state transitions. Lymphatic chains can go from state 1 to state 2, and so on, with some *transition probability*, and the probability that the system is in any state at time $t + 1$ depends only on the *present* state, the state of everything at time t, and *not* the history of how it got there.

If each lymphatic chain were independent of all the others, the probabilities would form a state *vector* with five components, one probability for each possible state of the lymphatic chain could be in. For each possible transition we would have some probability, p_{ij}, the conditional probability that the system is in state j at time $t + 1$ given that it is in state i at time t. Strictly speaking, this transition probability can depend on time. Processes in which the transition probabilities do *not* depend on time are *homogeneous*. In such cases, the transition probabilities form a matrix, and the relation between the state vector at time $t + 1$ and the state vector at time t is just multiplication of the state vector by the transition matrix, to get the new state vector.

In this paper, we introduce a new Markov chain model for nodal spread of head and neck cancer using data by T stage, tumor site and nodal stage to flexibly compare the output with patient data from surgical pathology of head and neck cancer. We decided to use the lateral tongue as our primary site of interest because it was a primary tumor for which we had a relatively large group of patients (50 patients) with which to find the parameters of the model, and were able to identify a number of studies in the literature that contained data by both T stage and lymph node involvement. To evaluate the accuracy of the model derived from the patient data, we systematically compare the predictions of the model for against the results found in the literature data.

Methods

Assumptions

We make a number of simplifying assumptions in building the current model. We assume that lymphatic chains are not "skipped" so that if disease is present in the fourth chain in the lymphatic path from the primary site, it is also present in the first three. Although skips do occur, they are relatively infrequent.[10] We assume that the process of primary growth and the process of dissemination from one lymphatic chain to the next are independent of each other and their rates are independent of time. Since the density of lymphatic channels varies greatly by primary sites, we assume that the probability of initial metastasis may be different for different first echelon lymphatic chains. However, as an initial simplifying assumption, once a tumor is within the lymphatic system, we assume that the probability of dissemination from one chain to the next along a lymphatic path is the same for all paths and all chains. We also make a simplifying assumption that the probability of growth from one T stage to the next is the same for all T stage transitions. We assume that the probability of diagnosing a tumor may change as the size and metastatic spread of the tumor increases. We start with these simplifying assumptions, and find out from comparing model predictions with data how to refine this set of assumptions as the model is further developed.

Structure

Instead of modeling each chain as having several states with varying amounts of tumor, and using the T-stage as a proxy for how many iterations to run in the initial model,[8] we propose a richer but simpler model: a single Markov chain that represents the patient's disease status using two layers of two dimensional array of states, indexed by T-stage for the primary tumor location and by the number of steps of metastasis along a lymphatic pathway as illustrated in Figure 1. The T-stage can take on 4 values, 1-4, corresponding to the standard clinical definition of T-stage for HNSCC. The metastatic progression along the lymphatics can be 0 for no metastasis, 1 for metastatic disease present in the first echelon of lymphatic vessels, 2 for disease present in the first and second echelons, and so on. For example, a patient with T-stage 2 and metastatic progression 2 has a primary tumor clinically defined as stage 2 and metastatic disease in the first two echelons of regional lymphatic nodes.

This describes a dynamic process whereby at each step a tumor can either grow in size to a larger T stage, metastasize further down the lymphatic pathway, or stay in the same state. With this model, given enough time, all tumors will invariably end up as the largest size with the most extensive metastasis. Of course, this is not what is actually observed in the clinical setting; at some point in this process the tumor is diagnosed, evaluated and a therapeutic intervention initiated. The size of tumor and degree of metastasis at the time of evaluation and/or management is what is typically

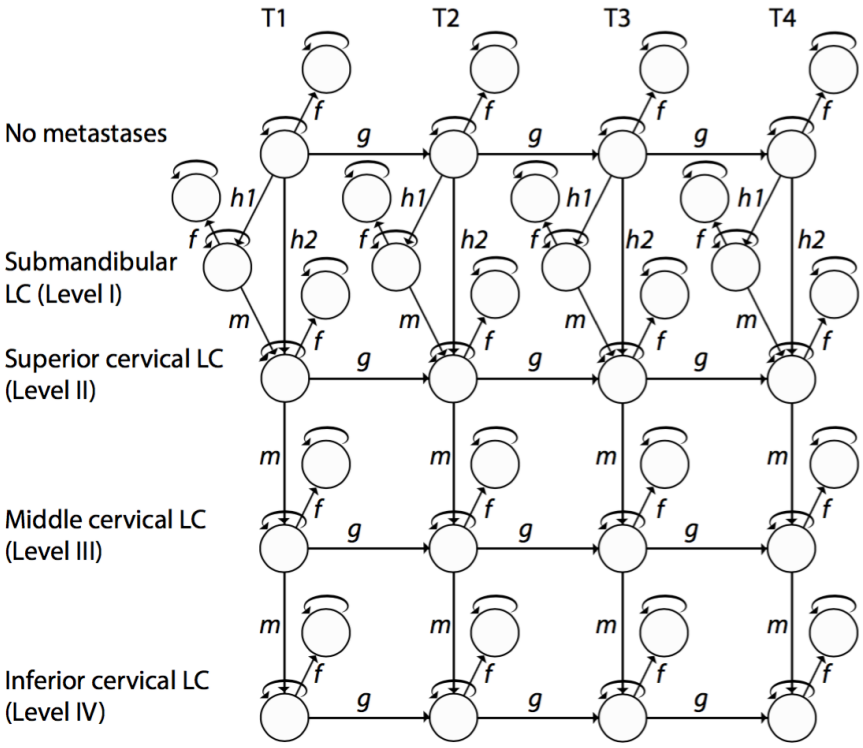

Figure 1: Diagram of two-dimensional model: T-stage is indexed across the top and depth of nodal spread along side. Roman numerals on the side refer to regional levels of the neck as per standard clinical terminology.

reported in the literature or clinical record. In order to model this process, we added an emission layer for each state, representing the probability of the tumor being diagnosed at that state. Once in the emission layer there is no further tumor growth or metastasis (the tumor has been diagnosed and recorded.) This approach provides several advantages. It allows us to model a clinical process that is inherent in the patient and literature datasets that we use to train and test the model.

The transition matrix for this set of states can be thought of as a four dimensional matrix indexed by the initial T-stage and lymphatic path depth, and the final T-stage and lymphatic path depth. Only stepwise transitions are hypothesized so the transition matrix is mostly zeros, and can be represented by a sum of delta functions. The definitions of parameters used in our Markov model are as follows: g represents the probability of primary tumor growth by one T-stage. m represents the probability of metastasis one step further down the lymphatic path. h_1 represents the probability of initial metastasis from primary site to one of the first echelon lymphatic chains, the Submandibular LC (Level I) in Figure 2. h_2 represents the probability of initial metastasis from primary site to the Superior cervical LC (Level II) as demonstrated in Figure 2, which is both a first echelon lymphatic chain via one pathway and a second echelon lymphatic chain from the Submandibular LC. f represents a linear function with two variables, α and β, the probability of moving from a node to its corresponding emission layer node.

We represent the probability of being in state s, c at time t as $P_{s,c}(t)$ and the Markov chain then consists of the successive time states, where each state can be computed from the previous state by Equation 1.

$$P_{s,c}(t+1) = \sum_{i=0,j=0}^{i=s,j=c} M_{s,c,i,j} P_{i,j}(t) \tag{1}$$

The sum is only taken up to the state indices of interest, since there is no contribution from a higher T-stage to a lower T-stage and there is no contribution from a downstream lymphatic chain to an upstream one.

Training set and test set

For our training set, we used data abstracted from the records of 50 patients who presented to the University of Washington head and neck tumor board over a three and half year time period with an initial diagnosis of non-treated

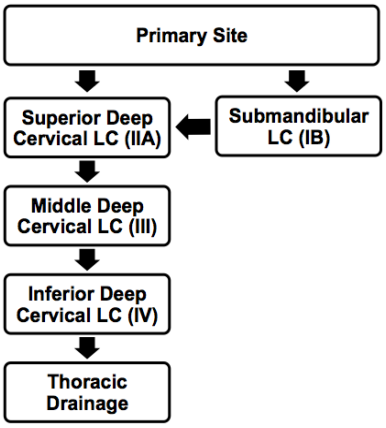

Figure 2: Diagram of lymphatic drainage pathways for the Lateral Tongue Tract. Arrows indicate sequential dissemination of metastatic tumor cells through lymphatic chains (LC).[12, 13, 14]

squamous cell carcinoma of the anterior tongue (excluding specific tumors of the base of tongue or ventral tongue.) This provided a dataset. Primary tumor stage was taken from the tumor board report and nodal involvement from the review of pathology reports of neck dissections. In some cases of low stage tumors (T_1 or T_2) without radiographic or clinical evidence of nodal involvement and very low suspicion of metastasis, a neck dissection was not performed. In these cases we assumed the absence of nodal metastasis. While the number of patients in the training set is smaller than some of the literature datasets, the patient dataset contains discrete information about the involvement of each nodal level at each T stage.

In the patient dataset that we used as a training set, the rate of metastasis was reported as the number of patients with a given T stage that had metastasis to a particular level of the neck, along with the number of total patients with that T stage. However, any individual patient may have metastasis to more than one level. In order to compare our model to the dataset, we converted our state probabilities to an analogous measurement. For each T stage, we determined the probability that a given echelon was involved with tumor by adding the probabilities of all states that included metastatic involvement of that echelon.

For our test sets, we selected four studies from the literature that record aggregated values for nodal involvement and T stage distribution. These studies were typically performed to test the utility of treatment modality, not necessarily to describe the patterns of lymph node metastasis. We chose two studies (Dogan, Dias)[5, 6] that provided aggregated information on all four potential lymph node levels. We also chose two studies (Lim, Sparano)[3, 4] which provided aggregated information on Levels I-III only. This was due to the fact that these studies utilized a type of neck dissection that does not include Level IV, due to a clinical decision that the probability of metastasis in these patients was too low to warrant removal of these lymph nodes. In these studies, we assumed that if Level IV was not treated then it did not contain metastases. (This correlates with our assumption in corresponding cases in the patient dataset.) While these literature studies do not provide discrete information about each individual nodal level by T stage, they have the advantage of larger numbers in some cases. Since each study draws patients from a somewhat different distribution of T stages, different studies allow us to test the predictive ability of our model across different T stage distributions.

Finding parameters

In order to execute the model, we need the parameters of m, g, h_1, h_2, α, and β values, in which m represents the probability of further metastasis along the lymphatic pathway, g represents the probability of primary tumor growth to a higher T stage, h_1 and h_2 represents the probability of initial metastasis to the two potential first echelon nodes, and α and β are coefficients in a linear function that represents the probability of diagnosing a tumor in that specific state. The strategy of finding parameters was to execute the model with a set of possible cases with a training dataset and get the optimal case where the output matrix is closest to the training dataset. We then identified the parameters based on the output of the case.

To generate a set of possible cases, we used a single layer grid search with a combination of m, g, h_1, h_2, α, and β values with the following ranges: m, g, h_1, and h_2, between 0 and 1 with a step size of 0.05 and α and β between 0 and 1 with a step size of 0.025. This generated $326,922,561 (= 21 \times 21 \times 21 \times 21 \times 41 \times 41)$ cases. We then excluded

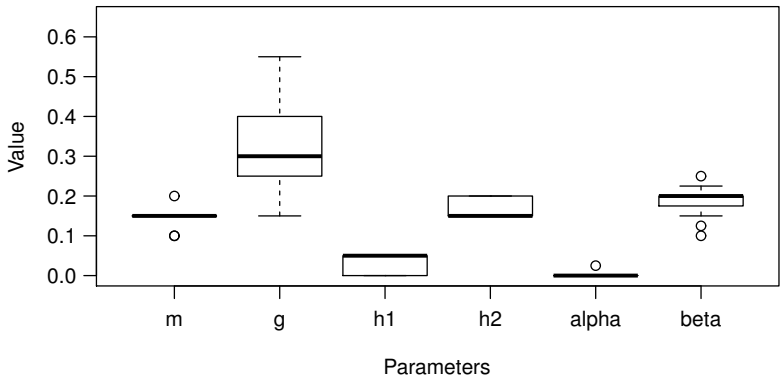

Figure 3: Variability of parameters among 18 sets of parameters that fit best with a training dataset based on RMS values. m represents the probability of further metastasis along the lymphatic pathway, g represents the probability of primary tumor growth to a higher T stage, h_1 and h_2 represents the probability of initial metastasis to the two potential first echelon nodes, and α and β are coefficients in a linear function that represents the probability of diagnosing a tumor in that specific state.

cases if the sum of the probabilities of the outgoing edges from each node was not 1 (one of the Markov chain rules).

After that, we judged closeness of the output of the case and training dataset by calculating the root mean square (RMS) error using the Equation 2. The distance between our model output and the training data is smaller when the RMS error is small. Let A and B be a matrix, a_{ij} and b_{ij} is an element with row ai and column j. C is the number of echelons and S is the number of T-stages.

$$rms(A, B) = \sqrt{\sum_{i=1}^{C}\sum_{j=1}^{S}(b_{ij} - a_{ij})^2} \tag{2}$$

Execution

We ran the model with four literature data as test datasets using the parameters, m, g, h_1, h_2, α, and β, we found from a training dataset. We ran our model until the sum of the probabilities on the emission layer becomes greater than 0.99. Prior to running the model, the initial probability matrix P used in the Markov chain model for the initial tumor site is given below:

$$P_{init} = \begin{pmatrix} 1.00 & 0.00 & 0.00 & 0.00 \\ 0.00 & 0.00 & 0.00 & 0.00 \\ 0.00 & 0.00 & 0.00 & 0.00 \\ 0.00 & 0.00 & 0.00 & 0.00 \\ 0.00 & 0.00 & 0.00 & 0.00 \end{pmatrix}$$

P_{11} has probability 1, indicating the site of our primary tumor. All other probabilities are 0, indicating that there is no prior metastasis or tumor growth. The model is then run for n iterations where n is the number of the states. The number of iterations was the number of the states because our model calculates the final probability for each state. For each iteration, the probability being in each state is calculated using the transition matrix that corresponds to our two-dimensional model as illustrated in Figure 1.

Results

Parameters

After systematic runs with a range of parameter values, we identified 18 out of $188,039$ (top 0.01 percent) combinations of parameters, m, g, h_1, h_2, α, and β, based on the RMS value. Since we aimed to find the parameters that fit most with a training dataset, The average values of the 18 sets of parameters are as follows: $m = 0.1473 \pm 0.0203$, $g = 0.325 \pm 0.0917$, $h_1 = 0.0278 \pm 0.0249$, $h_2 = 0.1667 \pm 0.0236$, $\alpha = 0.0014 \pm 0.0058$, and $\beta = 0.1889 \pm 0.0356$. The box plots in Figure 3 demonstrate the range and interquartile range of parameters, m, g, h_1, h_2, α, and β.

Table 1: Comparison of our model's predictions with patient data of the Lateral Tongue Tract when $m = 0.15$, $g = 0.4$, $h_1 = 0.05$, $h_2 = 0.2$, $\alpha = 0.0$, and $\beta = 0.175$. The numbers in the table demonstrate the number of patients for each site, one from our model and the other from the patient dataset.

	Model	Data	Model	Data	Model	Data	Model	Data
	$T1$		$T2$		$T3$		$T4$	
No Metastases	12.6	14	10.5	12	3.8	1	0.9	1
Submandibular LC (I)	2	1	3.4	1	1.8	3	0.7	0
Superior cervical LC (II)	4.6	3	8.1	5	4.5	8	1.8	2
Middle cervical LC (III)	0.9	2	2.1	5	1.4	4	0.7	1
Inferior cervical LC (IV)	0.2	1	0.4	0	0.3	3	0.2	2

Table 2: Comparison of our model's predictions with five external datasets, one patient dataset and four literature datasets of the Lateral Tongue Tract when $m = 0.15$, $g = 0.4$, $h_1 = 0.05$, $h_2 = 0.2$, $\alpha = 0.0$, and $\beta = 0.175$. The numbers in the table represent cumulative values across all T stage per nodal echelons.

	Model	Patient	Model	Lim[3]	Model	Dias[6]	Model	Sparano[4]	Model	Dogan[5]
No Metastases	27.8	28	32.9	15	129.4	105	28.4	32	37.3	40
Submandibular LC (I)	7.9	5	7.7	8	33.5	58	6.1	2	10.8	5
Superior cervical LC (II)	19	18	17.9	7	78.7	93	14.1	9	25.3	20
Middle cervical LC (III)	5.1	12	4.3	6	19.5	26	3.3	3	6.8	6
Inferior cervical LC (IV)	1.1	6	0.8	0	3.8	18	0.6	0	1.5	3

Model validation

The model was validated using data from four previously published original articles. Similar to the internally collected data used to train the model, datasets from published article only contained patients data for their initial presentation and excluded recurrent cancer. External datasets report information on T stage of the patient's the as well as the anatomical nodal echelon of metastasis. Unlike internally collected data, the previously published data is sparse and incomplete therefore staging and nodal echelon data is reported in aggregate. Thus, the model is tested against the cumulative values across all T stage per nodal echelons and the cumulative values across nodal echelons per T stage. Of note, of the five external datasets, two[3, 4] come from studies that where patients underwent a supra-omohyoid neck dissection and level IV and V information is not available. Given the clinical rationale for a supra-omohyoid neck dissection (extremely rare metastasis to level IV or V) it is reasonable to assume a zero values for all level IV and V metastasis probabilities.

In order to test our model prediction, we produced an output after running our model using the following set of parameters that fit best with a training dataset: $(m, g, h_1, h_2, \alpha, \beta) = (0.15, 0.4, 0.05, 0.2, 0.0, 0.175)$. We obtained the number of patients for each site and compared it with one from the patient datasets as shown in Table 1. For comparing our model predictions with other external datasets, we calculated cosine similarity to measure the similarity between our model output and each external dataset using the Equation 3. The cosine similarity between our model output and the training dataset is closer when the cosine similarity approaches to 1. Given those two vectors, A from our model output and B from a training dataset, the cosine similarity is defined as follows:

$$\cos(A, B) = \frac{A \cdot B}{\| A \| \| B \|} \tag{3}$$

Table 2 shows cumulative values across all T stage per nodal echelons from our model output and each external dataset. With the cumulative values, we created two vectors, A and B, each of which consists of cumulative values across all T stage per nodal echelons from our model output and external datasets, respectively. We then calculated the cosine similarity between our model output and each external dataset. Table 3 shows the cosine similarity values between our model prediction and each external dataset.

Discussion

We have proposed a novel Markov chain model for prediction of HNSCC tumor dissemination through the lymphatics of the head and neck. In establishing parameters, we focused primarily on a subset of HNSCC, the case in which the primary tumor arises in the lateral tongue region. As such, we were able to generate predictive probabilities using our

Table 3: Cosine similarity our model's predictions with one patient and four literature data of the Lateral Tongue Tract when $m = 0.15$, $g = 0.4$, $h_1 = 0.05$, $h_2 = 0.2$, $\alpha = 0.0$, and $\beta = 0.175$. The values of cosine similarity are given.

Dataset	Cosine Similarity
Patient data	0.969
Lim[3]	0.949
Dias[6]	0.967
Sparano[4]	0.975
Dogan[5]	0.984

model and validate them against known clinical data. Now that the foundations of our model have been established and tested, we can proceed in future work to expand the Markov chain model to include further subsets of HNSCC that arise from different primary sites in the upper aerodigestive tract. There are many such different permutations for metastasis along the lymphatics which we hope to ultimately be able to incorporate into an expanded version of our model. Additionally, we aim to refine our Markov chain model to account for factors such as potential contralateral tumor dissemination. Such factors could be addressed by adding new dimensions onto our existing array. Ultimately, once our Markov chain model is fully expanded, we hope to use it to accurately and precisely predict the extent of micro-metastases dissemination in all cases and subsets of HNSCC, thereby creating a powerful new tool that clinicians can use to provide necessary care to patients while minimizing the deleterious effects of over-irradiation.

Limitations

The primary site was chosen due to the relatively large number of patients in our dataset with anterior tongue primary tumors (not including the base of tongue.) Our model only considers ipsilateral metastasis. Contralateral metastasis can occur and we are working to incorporate bilateral metastases into our model. Our model does not include the possibility of skip metastasis. While skip metastases are relatively infrequent, we are investigating ways of incorporating the possibility of skip metastases into future models.

In regard to test and training sets, the literature datasets we used as test sets contain aggregated probabilities for both T stage and lymph node level. We compared the involvement of each nodal group in the test set to what was predicted by the model for the same T stage distribution of that test set. This is a limitation of the existing literature. The patient dataset we used does contain discrete (non aggregated) probabilities that we calculated for each T stage and lymph node level. However, the training set is relatively limited in size, which results in small numbers of observations particularly for more advanced tumors (since most tumors are treated before they reach an advanced stage.)

We assume that m is the same but we could add other parameters that release this assumption. We realize that this is likely an oversimplification and the model may be able to achieve better performance with more variables. Increasing the number of variables with the current amount of training data runs the risk of overfitting. A reasonable assumption is that the probability of tumor metastasizing between different nodal regions may have somewhat different values. However, the probability of tumor metastasizing from one specific nodal region to another specific nodal region is likely independent of the primary site (since all of these tumors are of the same histologic type.) Our future work is to build additional models for different primary sites that share all or part of the same lymphatic drainage pathways. This will allow us to use additional data to fit specific parameters that represent the probability of metastasis between specific lymphatic chains.

We also assume that the probability of growth is a constant parameter. As above, this is likely an oversimplification. However, the TNM tumor stage has been designed to divide each primary tumor site into four "clinically relevant" divisions, which span different primary sites. We therefore felt that this was a reasonable simplification as increasing the number of growth parameters carries the same risk of overfitting described above.

Acknowledgements

Research reported in this publication was supported by the National Library Of Medicine of the National Institutes of Health under Award Number R21-LM012075. The content is solely the responsibility of the authors and does not necessarily represent the official views of the National Institutes of Health. The first author (Jung) acknowledges support from the Korean Government Scholarship and Mogam Science Scholarship.

References

1. International Commission on Radiation Units and Measurements. Prescribing, Recording and Reporting Photon Beam Therapy. Bethesda, MD: International Commission on Radiation Units and Measurements; 1993. Report 50.

2. International Commission on Radiation Units and Measurements. Prescribing, Recording and Reporting Photon Beam Therapy (Supplement to ICRU Report 50). Bethesda, MD: International Commission on Radiation Units and Measurements; 1999. Report 62.

3. Lim YC, Lee JS, Koo BS, Kim SH, Kim YH, Choi EC. Treatment of contralateral N0 neck in early squamous cell carcinoma of the oral tongue: Elective neck dissection versus observation. Laryngoscope. 2006;116:461–465.

4. Sparano A, Weinstein G, Chalian A, Yodul M, Weber R. Multivariate predictors of occult neck metastasis in early oral tongue cancer. Otolaryngology - Head and Neck Surgery. 2004;131:472–476.

5. Dogan E, Cetinayak HO, Sarioglu S, Erdag TK, Ikiz AO. Patterns of cervical lymph node metastases in oral tongue squamous cell carcinoma: Implications for elective and therapeutic neck dissection. Journal of Laryngology and Otology. 2014;128:268–273.

6. Dias FL, Lima RA, Kligerman J, Farias TP, Soares JRN, Manfro G, et al. Relevance of skip metastases for squamous cell carcinoma of the oral tongue and the floor of the mouth. Otolaryngology - Head and Neck Surgery. 2006;134:460–465.

7. Phillips MH, Smith WP, Parvathaneni U, Laramore GE. Role of Positron Emission Tomography in the Treatment of Occult Disease in Head-and-Neck Cancer: A Modeling Approach. International Journal of Radiation Oncology, Biology and Physics. 2011;79(4):1089–1095.

8. Benson N, Whipple M, Kalet IJ. A Markov model approach to predicting regional tumor spread in the lymphatic system of the head and neck. In: AMIA Annual Symposium Proceedings. vol. 2006. American Medical Informatics Association; 2006. p. 31.

9. Kalet IJ. Principles of Biomedical Informatics. 2nd ed. Waltham, MA: Academic Press (Elsevier); 2013.

10. Gregoire V, Coche E, Cosnard G, Hamoir M, Reychler H. Selection and delineation of lymph node target volumes in head and neck conformal radiotherapy. Proposal for standardizing terminology and procedure based on the surgical experience. Radiotherapy and Oncologie. 2000;56:135–150.

11. Woolgar JA. Histological distribution of cervical lymph node metastases from introral/oropharyngeal squamous cell carcinomas. British Journal of Oral and Maxillofacial Surgery. 1999;37:175–180.

12. Fisch U. Lymphography of the Cervical Lymphatic System. London: W.B. Saunders Co.; 1968.

13. Mayerson HS. Lymph and the Lymphatic System. Springfield: Thomas Books; 1965.

14. Rusznyak I. Lymphatics and Lymph Circulation. New York: Pergamon Press; 1967.